

Supramolecular organisation of oligo(*p*-phenylenevinylene) at the air–water interface and in water

2 PERKIN

Pascal Jonkheijm, Michel Fransen, Albertus P. H. J. Schenning and E. W. Meijer *

Laboratory of Macromolecular and Organic Chemistry, Eindhoven University of Technology, P.O. Box 513, 5600 MB, Eindhoven, The Netherlands. E-mail: E.W.Meijer@tue.nl; Fax: 31 (0)40 2451036; Tel: 31 (0)40 2472655

Received (in Cambridge, UK) 3rd May 2001, Accepted 13th June 2001

First published as an Advance Article on the web 11th July 2001

Two novel chiral (bola)amphiphilic oligo(*p*-phenylenevinylene)s (OPVs) have been synthesised and fully characterised. Decoration of the hydrophobic OPV backbone with a hydrophilic tris[tetra(ethylene oxide)]benzene wedge on one side and a hydrophobic tris(alkoxy)benzene wedge on the other side, resulted in amphiphilic **OPV1**. In bolaamphiphile **OPV2**, two hydrophilic tris[tetra(ethylene oxide)]benzene wedges are connected at both ends of the OPV backbone. The organisation of the amphiphiles has been investigated at the air–water interface and in water. Langmuir monolayers of **OPV1** showed that these amphiphiles are perpendicularly oriented at the air–water interface. In the case of **OPV2**, the OPV units are lying flat on the subphase with the hydrophilic ethylene glycol wedges pointing into the water phase. In chloroform, the OPV derivatives are present as molecularly dissolved species. In water, the amphiphilic OPV derivatives aggregate in chiral stacks, as can be concluded from UV–vis, fluorescence and CD spectroscopy. Temperature dependent measurements showed for **OPV1** a transition at 50 °C from a chiral aggregated state to disordered aggregates. In the case of bolaamphiphilic **OPV2**, the transition at 55 °C between those states is a less cooperative process. The chiral order in the assemblies of the bolaamphiphiles can be influenced by the addition of salt.

Introduction

π -Conjugated oligomers are regarded as the ideal model compounds for understanding the electro-optical properties of π -conjugated polymers. Impressive advances in research have been achieved on π -conjugated materials¹ and have led towards a better understanding of the relationship between the desired functional properties and the enhanced supramolecular structure, by making use of its well-defined chemical structure and conjugation length.² Highly ordered local structures are the prerequisite for obtaining electronic properties such as high carrier mobility. Controlled organisation of π -conjugated oligomers has been achieved by using a suitable solvent–nonsolvent mixture,³ thermotropic and lyotropic liquid crystallinity^{4,5} hydrogen bonding motifs,^{6,7} and by block copolymers.⁸ Efficient macromolecular assembly of oligomers will become critically important to achieve new applications, molecular electronics providing the most outstanding prospect.⁹

Surfactant interactions are often used in nature to assemble molecules into large systems, such as membranes. This methodology has inspired chemists to synthesise a variety of artificial surfactants, *e.g.* amphiphiles, to construct well-defined assemblies in water and at the air–water interface.¹⁰ Remarkably, lipophilic interactions have rarely been applied in the supramolecular organisation of π -conjugated oligomers in contrast to amphiphilic π -conjugated polymers.¹¹ Recently, the self-assembly of α,ω -disubstituted sexithiophenes in butanol and water has been reported.¹² Alternating α -oligothiophene blocks with poly(ethylene oxide) blocks have been synthesised and the oligothiophenes aggregate in a 83% water–dioxane mixture in a face-to-face manner.¹³ Oligo(*p*-phenylenevinylene) (OPV) has been functionalised with ethylene glycol chains¹⁴ and pendant ethylene glycol dendrons¹⁵ showing superstructures in THF–water^{14a} and water^{14b} and at the air–water interface, respectively. Monolayers have also recently been constructed from amphiphilic OPVs containing a pyridine or diaminotriazine headgroup to obtain controllable organisation at the air–water

interface.¹⁶ The Langmuir–Blodgett technique can be used to prepare light-emitting diodes (LED) that show linear polarisation of the emitted light.¹⁷

Here, we report the synthesis of two novel chiral (bola)amphiphilic OPV's (Scheme 1, **OPV1** and **OPV2**) as an extension of our work on the fully aliphatic OPV oligomers of different lengths.¹⁸ Amphiphile **OPV1** consists of a hydrophobic OPV tetrameric core with, at one end a hydrophobic trialkoxybenzene wedge and, at the other end, a hydrophilic tris[tetra(ethylene oxide)]benzene wedge. Bolaamphiphile **OPV2** contains a hydrophobic pentameric OPV core, substituted with two hydrophilic tris[tetra(ethylene oxide)]benzene wedges at both ends. We have chosen chiral amphiphiles because a stereocenter in the side-chain has been proven to be a very informative probe in studying the expression of chirality at the supramolecular level.¹⁹ The organisation of the OPV amphiphiles has been studied at the air–water interface and in water.

Experimental

General methods: ¹H NMR and ¹³C NMR spectra were recorded at room temperature on a Varian Gemini 300 or a Varian Mercury 400. Chemical shifts are given in ppm (δ) relative to tetramethylsilane. Abbreviations used are s = singlet, d = doublet, dd = double doublet, t = triplet and m = multiplet. Infrared spectra were run on a Perkin Elmer 1600 FT-IR spectrometer. MALDI-TOF MS spectra were measured on a Perspective DE Voyager spectrometer utilizing an α -cyano-4-hydroxycinnamic acid matrix. Elemental analyses were carried out on a Perkin Elmer 2400. Differential scanning calorimetry measurements were performed on a Perkin Elmer DSC Pyris 1 at a heating rate of 40 °C min⁻¹. UV–vis and fluorescence spectra were performed on a Perkin Elmer Lambda 40 spectrophotometer and a Perkin Elmer LS-50 B. CD spectra were recorded on a JASCO J-600 spectropolarimeter. A description of the CPL apparatus can be found in the literature.²⁰

The aqueous solutions for optical measurements were prepared *via* a methanol injection method. The amphiphiles were dissolved in 50 μL methanol and this solution was injected into 5 mL demineralised water. After evaporation of the methanol, the temperature dependent optical spectra were recorded. The time between two measurements was 30 min.

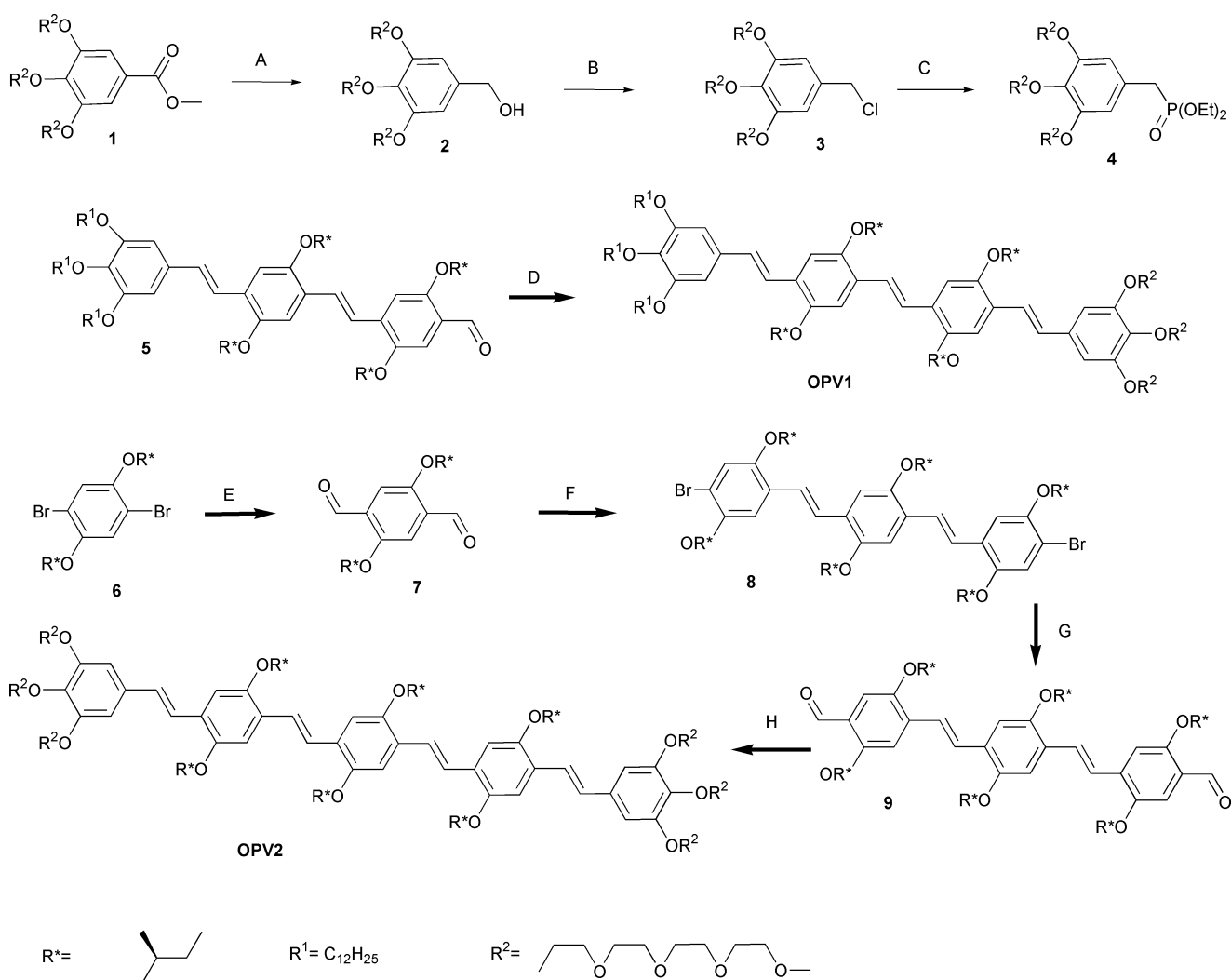
Monolayer experiments were performed with a KSV-5000 LB instrument placed on an anti-vibration table in a controlled atmosphere room. 10 μL of a chloroform solution (0.48 mM **OPV1** and 0.27 mM **OPV2**) was spread onto the subphase (micro-filtered de-ionised water, resistivity = 18.2 $\text{M } \Omega \text{ cm}$) at 20 $^{\circ}\text{C}$. The Langmuir film compression (30 mm min^{-1}) started 30 minutes after spreading. The surface pressure was measured using the Wilhelmy plate method with plates made of filter paper. Brewster angle microscope experiments were carried out with a NFT BAM1 instrument, manufactured by Nano Film Technology, Göttingen, which was equipped with a 10 mV He-Ne laser (beam diameter of 0.68 mm, 632.8 nm). Materials: methyl 3,4,5-tris(2-{2-[2-(2-methoxyethoxy)ethoxy]ethoxy}ethoxy)benzoate **1**, (*E,E*)-4-{4-[3,4,5-tris(dodecyloxy)styryl]-2,5-bis[(*S*)-2-methylbutoxy]styryl}-2,5-bis[(*S*)-2-methylbutoxy]benzaldehyde⁷ **5**, diethyl {2,5-bis[(*S*)-2-methylbutoxy]-4-bromobenzyl}phosphonate²¹ and 2,5-bis[(*S*)-2-methylbutoxy]-1,4-dibromobenzene²² **6** were synthesised according to literature procedures. All solvents were of AR quality and chemicals were used as received. BioBeads S-XI Beads were obtained from Bio-Rad Laboratories.

3,4,5-Tris(2-{2-[2-(2-methoxyethoxy)ethoxy]ethoxy}ethoxy)-benzyl alcohol (**2**)

Under an argon atmosphere, a solution of **1** (17.59 g, 23.30 mmol) in 100 mL dry THF was added dropwise to a suspension of LiAlH_4 (0.97 g, 25.60 mmol) in 20 mL dry THF at 0 $^{\circ}\text{C}$. After refluxing overnight, the solution was poured on 100 mL crushed ice. Sulfuric acid (60 mL, 10%) was added and the aqueous layer was extracted twice with dichloromethane. The collected organic layers were washed with brine and dried (Na_2SO_4), filtrated and evaporated to dryness, resulting in 16.09 g (95%) of **2**. $^1\text{H NMR}$ (300 MHz, CDCl_3): δ 3.18 (s, 6H, OCH_3), 3.19 (s, 3H, OCH_3), 3.35–3.70 (m, 42H, OCH_2), 3.95 (m, 6H, ArOCH_2), 4.38 (s, 2H, ArCH_2OH), 6.42 (s, 2H, ArH); $^{13}\text{C NMR}$ (100 MHz, CDCl_3): δ 25.0, 58.3, 63.9, 67.2, 68.2, 69.2, 69.8, 70.0, 70.1, 71.3, 71.7, 105.6, 136.7, 136.7, 152.0; MALDI-TOF MS ($M = 726.86$) $m/z = 749.57$ [$M + \text{Na}$] $^+$.

3,4,5-Tris(2-{2-[2-(2-methoxyethoxy)ethoxy]ethoxy}ethoxy)-benzyl chloride (**3**)

To a stirred solution of **2** (10.0 g, 13.76 mmol) in 25 mL dry dichloromethane, were added three drops of DMF and thionyl chloride (4.9 g, 41.3 mmol). The progress of the reaction was monitored by TLC. After 1 h, the reaction was completed and the solvent was evaporated. The residue (10.0 g, 13.42 mmol) was not further purified. $^1\text{H NMR}$ (400 MHz, CDCl_3): δ 3.25



Scheme 1 A) LiAlH_4 , 8 h, 0 $^{\circ}\text{C}$. B) DCM, SOCl_2 , 1 h. C) $\text{PO}(\text{Et})_3$, 8 h, 160 $^{\circ}\text{C}$. D and H) DMF–THF, **4**, $\text{KOC}(\text{CH}_3)_3$, 8 h. E and G) DME, *n*-BuLi, –10 $^{\circ}\text{C}$, 1 h. F) DMF, $\text{KOC}(\text{CH}_3)_3$, diethyl {2,5-bis[(*S*)-2-methylbutoxy]-4-bromobenzyl}phosphonate, 3 h, rt.

(s, 6H, OCH₃), 3.26 (s, 3H, OCH₃), 3.43–3.75 (m, 42H, OCH₂), 4.10 (m, 6H, ArOCH₂), 4.40 (s, 2H, ArCH₂Cl), 6.53 (s, 2H, ArH); ¹³C NMR (100 MHz, CDCl₃): δ 46.2, 58.5, 68.5, 69.3, 70.0, 70.1, 70.2, 70.4, 71.5, 71.9, 107.9, 132.3, 138.0, 152.2.

Diethyl (3,4,5-tris(2-{2-[2-(2-methoxyethoxy)ethoxy]ethoxy}benzyl)phosphonate (4)

A mixture of triethyl phosphite (13.85 g, 83.4 mmol) and 3 (10.00 g, 13.42 mmol) was stirred at 160 °C for 8 h. During this time, ethyl chloride was distilled from the reaction mixture. Subsequently, the mixture was cooled to 70 °C and the excess of triethyl phosphite was distilled under reduced pressure. The product was used without further purification: ¹H NMR (300 MHz, CDCl₃) δ 1.21 (t, 6H, OCH₂CH₃), 3.02 (d, 2H, ArCH₂), 3.34–3.80 (m, 51H, OCH₂, OCH₃), 3.98 (m, 4H, POCH₂), 4.10 (m, 6H, ArOCH₂), 6.53 (s, 2H, ArH); ³¹P NMR (400 MHz, CDCl₃) δ 27.37.

(*E,E,E*)-1-{4-[3,4,5-Tris(dodecyloxy)styryl]-2,5-bis[(*S*)-2-methylbutoxy]phenyl}-2-{4-[3,4,5-tris(2-{2-[2-(2-methoxyethoxy)ethoxy]ethoxy}ethoxy)styryl]-2,5-bis[(*S*)-2-methylbutoxy]phenyl}ethene (OPV1)

Phosphonate 4 (77 mg, 0.09 mmol) was dissolved in 10 mL anhydrous DMF. Potassium *tert*-butoxide (60 mg, 0.54 mmol) was added to the solution under an argon atmosphere. After 15 minutes, a solution of aldehyde 5 (100 mg, 0.08 mmol) in 15 mL THF was added dropwise to the reaction mixture. The solution was stirred overnight at room temperature. 100 mL HCl (6 M) was added and the aqueous layer was extracted three times with chloroform. The collected organic layers were washed with HCl (3 M) and dried over MgSO₄, filtrated and evaporated to dryness. The crude mixture was purified by column chromatography (silica gel, 3% methanol in CH₂Cl₂) and dried thoroughly over P₂O₅ to afford 111 mg (73%) of OPV1 as a red wax. Mp 51 °C; ¹H NMR (400 MHz, CDCl₃): δ 0.90 (t, 9H, (CH₂)₉CH₃), 1.02 (m, 12H, CH₃), 1.13 (m, 12H, CH₃), 1.3 (m, 54H, OCH₂CH₂(CH₂)₉CH₃), 1.5 (m, 8H, CH₂), 1.7 (m, 2H, CH₂), 1.85 (m, 4H, CH), 1.96 (m, 4H, CH₂), 3.38 (s, 6H, OCH₃), 3.39 (s, 3H, OCH₃), 3.53–3.77 (m, 42H, OCH₂), 3.82–3.93 (m, 6H, OCH₂(CH₂)₁₀CH₃), 4.01 (m, 8H, OCH₂-CH(CH₃)CH₂CH₃), 4.21 (m, 6H, ArOCH₂), 6.76 (s, 2H, ArH), 6.78 (s, 2H, ArH), 7.05 (d, 2H, *J* = 16.2 Hz, ArCH=CH), 7.11 (d, 2H, *J* = 5.1 Hz, ArCH=CH), 7.21 (s, 2H, ArH), 7.36 (d, *J* = 12.4 Hz, 1H, ArCH=CH), 7.41 (d, 1H, *J* = 12.4 Hz, ArCH=CH), 7.53 (s, 2H, ArH); ¹³C NMR (100 MHz, CDCl₃) δ 11.69, 11.71, 11.76, 14.34, 17.02, 17.06, 17.09, 22.92, 26.36, 26.44, 26.62, 29.60, 29.63, 29.66, 29.85, 29.89, 29.94, 29.97, 29.99, 30.57, 32.15, 32.17, 35.22, 35.31, 35.38, 59.24, 68.86, 69.03, 69.31, 69.84, 70.00, 70.73, 70.74, 70.82, 70.90, 71.06, 72.15, 72.65, 73.78, 74.37, 74.41, 74.65, 105.29, 106.33, 109.99, 110.12, 110.65, 111.00, 122.73, 122.79, 122.9, 123.35, 126.75, 127.02, 127.64, 127.79, 128.61, 128.79, 133.46, 133.93, 138.36, 151.25, 151.30, 151.38, 152.97, 153.47; MALDI-TOF MS (*M* = 1900.73) *m/z* = 1900.43 [M], 1923.46 [M + Na]⁺, 1941.58 [M + K]⁺. Anal. Calcd. for C₁₁₃H₁₉₀O₂₂: C 71.41, H 10.08. Found: C 71.62, H 9.96%.

2,5-Bis[(*S*)-2-methylbutoxy]-1,4-diformylbenzene (7)

Under an argon atmosphere 36.75 mL of 1.6 M *n*-butyllithium in hexane were added dropwise to a solution of dibromide 6 (10 g, 24.5 mmol) in 200 mL dry ether at –10 °C. During the first 5 min 4.55 mL of dry DMF were added and a gel was formed. After stirring for 2.5 h the reaction mixture was poured into 200 mL HCl (6 M) and extracted with ether (150 mL). The organic layer was washed 3 times with 200 mL HCl (1 M), then with 300 mL water, followed by a saturated NaHCO₃ solution (300 mL). The organic layer was dried over MgSO₄, filtrated and evaporated to dryness. The crude mixture was purified

by column chromatography (silica gel, hexane–toluene 1:1). The first fraction appeared to be the monoaldehyde and the dialdehyde was removed from the column by eluting it with chloroform. Recrystallisation from hexane yielded 7 (3.93 g, 52%). ¹H NMR (300 MHz, CDCl₃): δ 0.97 (t, 6H), 1.05 (d, 6H), 1.35 (m, 2H), 1.60 (m, 2H), 1.90 (m, 2H), 3.8 (m, 4H), 7.44 (s, 2H, ArH), 10.54 (s, 2H); ¹³C NMR (100 MHz, CDCl₃): δ 11.24, 16.53, 26.08, 34.68, 73.88, 111.55, 129.29, 155.32, 189.30.

(*E,E*)-1,4-Bis{4-bromo-2,5-bis[(*S*)-2-methylbutoxy]styryl}-2,5-bis[(*S*)-2-methylbutoxy]benzene (8)

Dialdehyde 7 (4.80 g, 15.69 mmol) was dissolved in 100 mL dry DMF and slowly added under an argon atmosphere to a solution of diethyl {2,5-bis[(*S*)-2-methylbutoxy]-4-bromobenzyl}phosphonate (16.94 g, 35.29 mmol) and potassium *tert*-butoxide (3.96 g, 35.68 mmol) in 220 mL dry DMF and THF (1:1 mixture). After stirring for 3 h at room temperature, the mixture was poured into ice and 250 mL HCl (6 M) was added and extracted with chloroform. The organic layer was washed several times with 250 mL HCl (3 M) and again with 200 mL water and subsequently dried over MgSO₄, filtered and evaporated to dryness. The crude mixture was purified by column chromatography (silica gel, DCM–pentane 1:1). After recrystallisation from ethanol, 8.00 g (53%) of 8 was obtained. ¹H NMR (300 MHz, CDCl₃): δ 1.00 (m, 18H, CH₃), 1.10 (m, 18H, CH₃), 1.36 (m, 6H, CH₂), 1.65 (m, 6H, CH), 1.95 (m, 6H, CH₂), 3.78–3.94 (m, 12H, OCH₂), 7.11 (s, 2H, ArH), 7.17 (s, 2H, ArH), 7.18 (s, 2H, ArH), 7.44 (d, 2H, *J* = 16.7 Hz, ArCH=CH), 7.52 (d, 2H, *J* = 16.7 Hz, ArCH=CH); ¹³C NMR (100 MHz, CDCl₃): δ 11.33, 11.43, 16.59, 16.73, 16.79, 26.12, 26.29, 26.36, 34.84, 34.95, 35.01, 74.21, 74.47, 74.74, 110.10, 110.70, 111.47, 118.01, 122.38, 123.39, 127.26, 149.98, 150.97, 151.09; MALDI-TOF MS (*M* = 956.6) *m/z* = 956.6 [M]; IR (KBr): ν (cm⁻¹) = 663, 717, 737, 772, 815, 855, 876, 916, 971, 982, 1027, 1048, 1200, 1236, 1289, 1325, 1344, 1388, 1419, 1462, 1500, 1563, 2050, 2874, 2920, 2959, 3060; Anal. Calcd. for C₅₂H₇₆O₆Br₂: C 65.33, H 8.00. Found: C 65.03, H 7.75%.

(*E,E*)-1,4-Bis{4-formyl-2,5-bis[(*S*)-2-methylbutoxy]styryl}-2,5-bis[(*S*)-2-methylbutoxy]benzene (9)

Dibromide 8 (2.00 g, 2.09 mmol) was dissolved in 20 mL THF. The solution was cooled to –10 °C and 2.3 mL of a 2.5 M *n*-butyllithium solution in hexane were added slowly. After stirring for 5 min the cooling bath was removed and 1 mL dry DMF was added dropwise. The reaction mixture was stirred for another hour at room temperature. After addition of 100 mL HCl (6 M), the organic layer was washed with water (2 times 150 mL), a saturated NaHCO₃ solution (150 mL) and again with water (150 mL). The organic layer was dried over MgSO₄ and the solvent was evaporated. The residue was purified by column chromatography (silica, CH₂Cl₂–pentane 1:1) and recrystallization from heptane yielded 1.23 g (69%) 9. ¹H NMR (300 MHz, CDCl₃): δ 1.00 (m, 18H, CH₃), 1.10 (m, 18H, CH₃), 1.36 (m, 6H, CH₂), 1.65 (m, 6H, CH), 1.95 (m, 6H, CH₂), 3.81–4.03 (m, 12H, OCH₂), 7.24 (s, 2H, ArH), 7.26 (s, 2H, ArH), 7.35 (s, 2H, ArH), 7.54 (d, 2H, *J* = 16.8 Hz, ArCH=CH), 7.68 (d, 2H, *J* = 16.8 Hz, ArCH=CH), 10.5 (s, 2H, CH=O); ¹³C NMR (100 MHz, CDCl₃): δ 11.33, 11.43, 16.59, 16.73, 16.79, 26.12, 26.29, 26.36, 34.84, 34.95, 35.01, 73.70, 73.83, 74.12, 109.73, 110.19, 122.50, 123.11, 126.25, 127.42, 134.95, 150.67, 151.33, 156.38, 189.04; MALDI-TOF MS (*M* = 855.21) *m/z* = 854.49 [M]⁺; IR (KBr): ν /cm⁻¹ = 672, 723, 774, 814, 851, 874, 915, 970, 1007, 1041, 1124, 1152, 1200, 1263, 1343, 1390, 1423, 1463, 1504, 1595, 1668 (C=O), 2040, 2858, 2928, 2959, 3064. Anal. Calcd. for C₅₄H₇₈O₈: C 75.94, H 9.21. Found: C 75.62, H 9.46%.

(*E,E,E,E*)-1,4-Bis{4-[3,4,5-tris(2-{2-[2-(2-methoxyethoxy)ethoxy]ethoxy}styryl)-2,5-bis[(*S*)-2-methylbutoxy]styryl]-2,5-bis[(*S*)-2-methylbutoxy]benzene (OPV2)

Under an argon atmosphere, phosphonate **4** (925 mg, 1.08 mmol) was dissolved in 10 ml anhydrous DMF and potassium *tert*-butoxide (310 mg, 2.77 mmol) was added. After 15 minutes, a solution of dialdehyde **8** (310 mg, 0.36 mmol) in 7.5 mL THF was added dropwise to the reaction mixture. The solution was stirred overnight at room temperature. 100 mL HCl (6 M) was added and the aqueous layer was extracted three times with chloroform. The collected organic layers were washed with HCl (3 M) and dried over MgSO₄, filtrated and evaporated to dryness. The crude mixture was purified by column chromatography (silica gel) with eluents hexane–ethyl acetate (2:1) and CH₂Cl₂–ethanol (97:3) and, subsequently, Bio-Beads column chromatography (CH₂Cl₂) was performed. Thorough drying over P₂O₅ afforded 435 mg (54%) of **OPV2** as an orange wax. Mp 82 °C; ¹H-NMR (400 MHz, CDCl₃): δ 1.00 (m, 18H, CH₃), 1.10 (m, 18H, CH₃), 1.36 (m, 6H, CH₂), 1.65 (m, 6H, CH), 1.95 (m, 6H, CH₂), 3.36 (s, 12H, OCH₃), 3.39 (s, 6H, OCH₃), 3.5–3.8 (m, 84H, OCH₂), 3.8–3.9 (m, 12H, OCH₂CH(CH₃)CH₂CH₃), 4.21 (m, 12H, OCH₂), 6.76 (s, 4H, ArH), 7.03 (d, 2H, *J* = 16.4 Hz, ArCH=CH), 7.08 (s, 2H, ArH), 7.19 (s, 4H, ArH), 7.34 (d, 2H, *J* = 16.4 Hz, ArCH=CH), 7.52 (s, 4H, ArCH=CH); ¹³C NMR (400 MHz, CDCl₃): δ 11.33, 11.43, 16.81, 16.85, 26.38, 34.95, 35.01, 35.14, 59.00, 68.80, 69.77, 70.49, 70.53, 70.58, 70.59, 70.64, 70.65, 70.82, 71.91, 72.38, 74.15, 74.23, 74.43, 106.12, 109.83, 109.95, 110.75, 122.56, 122.75, 123.12, 126.50, 127.40, 127.59, 128.36, 133.69, 138.22, 151.03, 151.10, 151.20, 152.73; MALDI-TOF MS (*M* = 2240.89) *m/z* = 2239.94 [M]⁺, 2262.92 [M + Na]⁺, 2278.91 [M + K]⁺; IR (KBr): ν /cm⁻¹ = 663, 692, 731, 773, 810, 852, 965, 1044, 1103, 1201, 1247, 1289, 1349, 1387, 1421, 1462, 1505, 1579, 2050, 2873, 2920, 2958, 3059. Anal. Calcd. for C₁₂₂H₁₉₈O₃₆: C 65.39, H 8.91. Found: C 65.27, H 9.05%.

Results and discussion

Synthesis and characterisation

Optically active (bola)amphiphilic π -conjugated oligomers **OPV1** and **OPV2** (Scheme 1) were synthesised from the precursor diethyl [3,4,5-tris(2-{2-[2-(2-methoxyethoxy)ethoxy]ethoxy}benzyl)phosphonate], **4**. The synthesis of the precursor required three steps starting from methyl 3,4,5-tris[tetra(ethylene oxide)]benzoate, **1**. Reduction by LiAlH₄ of **1** afforded the corresponding alcohol derivative **2**. Chlorination of **2** in refluxing thionyl chloride with a catalytic amount of DMF yielded chloride derivative **3**. The obtained product was subsequently converted to **4** by performing a Michaelis–Arbuzov reaction with triethyl phosphite. Pure **OPV1** was obtained *via* a Wittig–Horner coupling reaction of aldehyde derivative **5** with **4**. Compound **OPV2** was synthesised starting from the dibromide derivative **6**. Substitution of the bromines by formyl groups, by reaction with *n*-BuLi in DMF according to the Bouveault method, resulted in pure **7**. Wittig–Horner coupling of **7** with diethyl {2,5-bis[(*S*)-2-methylbutoxy]-4-bromobenzyl}phosphonate yielded dibromide OPV derivative **8** which was subsequently converted to the dialdehyde **9** according to the same procedure as applied for **7**. After the coupling of **9** with **4**, bolaamphiphile **OPV2** was isolated. Both amphiphiles, **OPV1** and **OPV2**, were fully characterised by ¹H NMR, ¹³C NMR, IR spectrometry, MALDI-TOF mass spectrometry and elemental analysis.

Compounds **OPV1** and **OPV2** melt at 51 and 82 °C, respectively. Both amphiphiles are highly soluble in organic solvents such as THF, chloroform, and methanol. The UV-Vis spectra of **OPV1** and **OPV2** show broad absorption π - π^* bands at λ_{max} = 434 and 450 nm, respectively in chloroform solutions

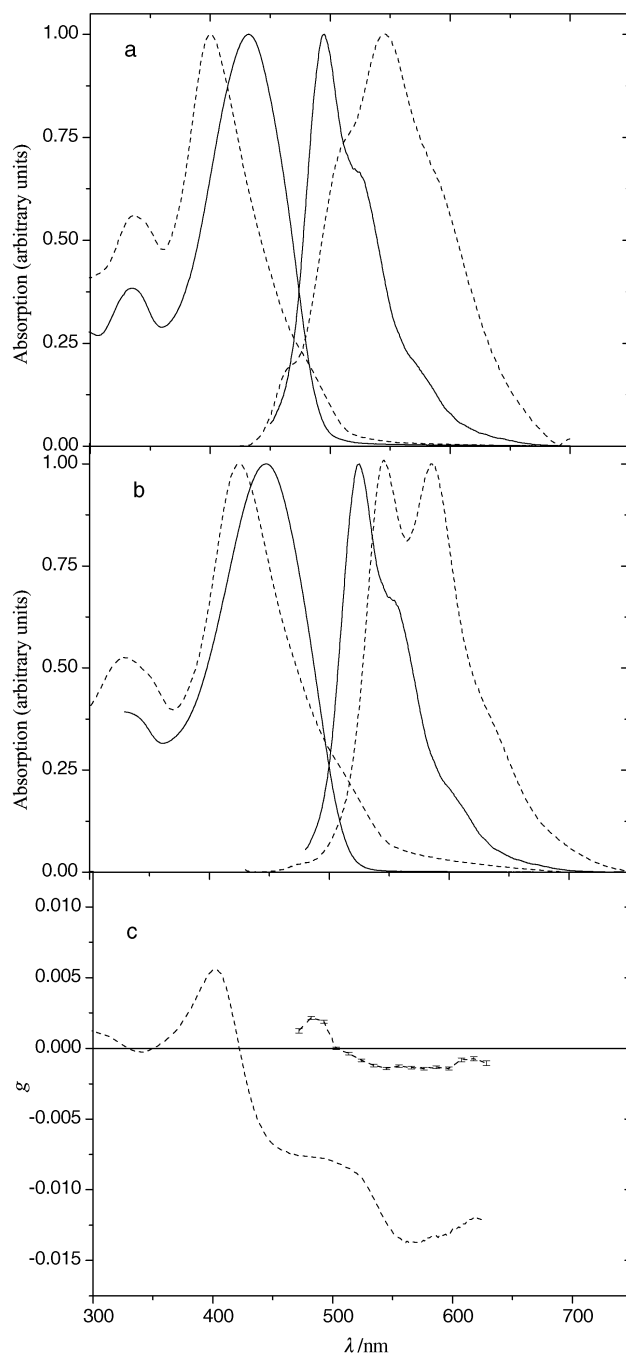


Fig. 1 Normalized UV-Vis and fluorescence spectra at 20 °C in chloroform (solid lines) and water (dashed lines) for a) **OPV1**, b) **OPV2** and c) circular polarisation in absorption (g_{abs}) and luminescence (g_{lum}) in water for **OPV2**.

(Fig. 1). The fluorescence maxima in chloroform are positioned at λ_{max} = 495 for **OPV1** and 525 nm for **OPV2** (Fig. 1). The absorption and fluorescence maxima are typical for a molecularly dissolved OPV tetramer and pentamer, respectively.¹⁸ The lack of a Cotton effect in chloroform supports the supposition that both amphiphiles are molecularly dissolved.³

Organisation at the air–water interface

In order to organise our amphiphiles into monolayers, **OPV1** and **OPV2** were spread on the air–water interface. The pressure–area isotherms (Fig. 2) display in both cases a slow increase in surface pressure with an onset of 375 and 750 Å² molecule⁻¹ for **OPV1** and **OPV2**, respectively. In the case of **OPV1** a collapse was found at a pressure of π = 45 mN m⁻¹ and a mean molecular area of 84 Å² molecule⁻¹ is obtained by extrapolating the steep rise in the condensed region to zero

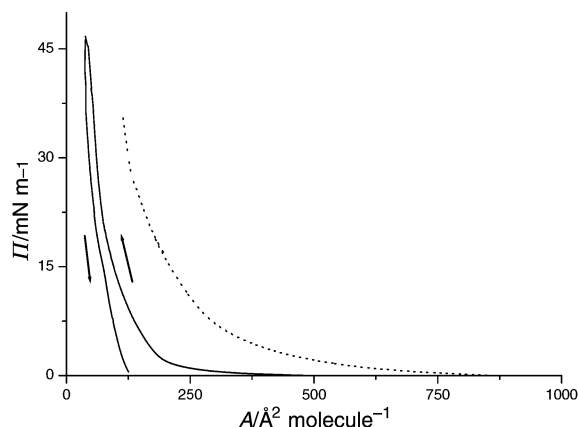


Fig. 2 Surface pressure–area (π - A) isotherms of **OPV1** (solid line) and **OPV2** (dotted line) obtained at 20 °C.

pressure. This value is similar to related OPV amphiphiles¹⁶ indicating that **OPV1** is perpendicularly oriented at the air–water interface. A large hysteresis was found in the isotherm suggesting monolayers with low stability (Fig 2). This behaviour is remarkably different from that of the related amphiphilic OPVs.¹⁶ The instability may be caused by the intrinsic flexibility of the tris[tetra(ethylene oxide)]benzene wedges. In the case of **OPV2**, Brewster angle microscopy (BAM) showed a homogeneous film after spreading, and small islands were formed at a pressure of $\pi = 12 \text{ mN m}^{-1}$. Unlike **OPV1**, the monolayers formed from **OPV2** show a flat rise in pressure with large hysteresis. This enlarged instability can be associated with the different orientation of this molecule at the air–water interface. Presumably, the OPV units are lying flat on the subphase with the hydrophilic ethylene glycol wedges pointing into the water. In such an orientation, an earlier onset of the pressure is expected while π - π stacking is unfavourable resulting in the formation of less stable monolayers.

Organisation in water

In comparison with chloroform solutions, the UV-Vis absorption spectra in water are blue shifted to $\lambda_{\text{max}} = 402 \text{ nm}$ (**OPV1**) and to $\lambda_{\text{max}} = 426 \text{ nm}$ (**OPV2**) with the appearance of a vibronic shoulder at 467 and 486 nm, respectively (Fig. 1). The fluorescence is strongly quenched in water and red shifted to $\lambda_{\text{em,max}} = 548 \text{ nm}$ (**OPV1**) and $\lambda_{\text{em,max}} = 546$ and 585 nm (**OPV2**). The absorption and fluorescence data show that the OPV oligomers are aggregated.³ A bisignate Cotton effect (Fig. 3) was observed for **OPV1** in water at the π - π^* band with a positive Cotton effect at $\lambda = 384 \text{ nm}$ ($g_{\text{abs}} = 6.3 \times 10^{-4}$) and a negative Cotton effect at $\lambda = 424 \text{ nm}$ ($g_{\text{abs}} = -1.1 \times 10^{-3}$). The zero-crossing of the CD signal ($\lambda = 400 \text{ nm}$) lies close to the absorption maximum of the chromophore. Compound **OPV2** also gave a strong bisignate Cotton effect with a positive and negative sign at $\lambda = 405 \text{ nm}$ ($g_{\text{abs}} = 5.6 \times 10^{-3}$) and $\lambda = 447 \text{ nm}$ ($g_{\text{abs}} = -6.5 \times 10^{-3}$), respectively with the CD signal going through zero at $\lambda = 423 \text{ nm}$, near the absorption maximum of the π - π^* band. Additionally, circular polarization of the luminescence (CPL) of **OPV2** in water was measured (Fig. 1). The CPL effect, expressed as the dissymmetry factor (g_{lum}), was found to be negative and essentially constant over the emission band for **OPV2** between 500 and 630 nm ($g_{\text{lum}} = -1.4 \times 10^{-3}$) and identical to the sign of g_{abs} in the long wavelength tail of the absorption. The observations in CD and CPL strongly indicate that the exciton coupling for the amphiphilic OPVs originates from aggregated OPV-oligomers assembled in chiral supra-molecular stacks.²³ The aggregates possess not only a chiral ground state but a chiral excited state as well. The magnitude of g_{lum} , however, is considerably lower than the maximum value of g_{abs} . This difference might be explained in terms of luminescent

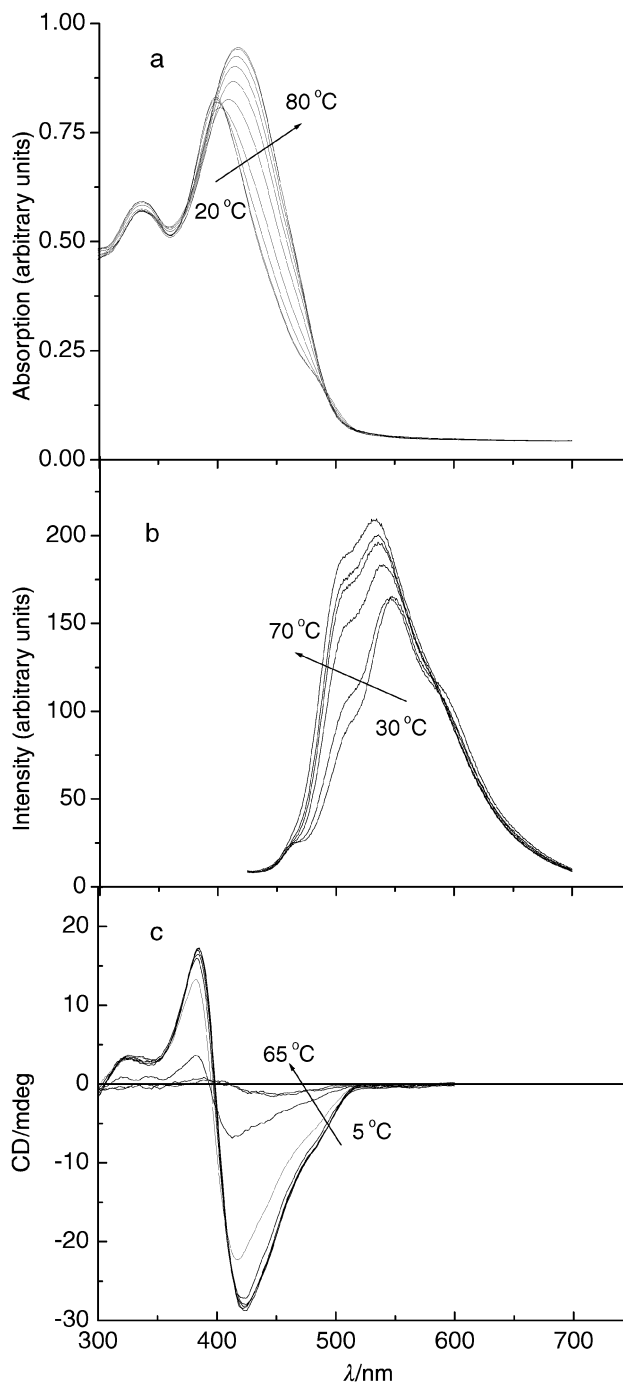


Fig. 3 Temperature dependent a) UV-Vis, b) fluorescence and c) CD measurements for **OPV1** at $1.6 \times 10^{-5} \text{ mol L}^{-1}$ in water.

trap sites.²⁰ Since the g_{abs} of the aggregates is negative in the 475–500 nm range, the aggregated molecules can cause an artefact in the CPL measurement by preferentially absorbing right circularly polarised light emitted by the non-aggregated molecules and, hence, the emitted light shows a positive g_{lum} below 500 nm.²

The aggregation process of both amphiphiles was further investigated by temperature dependent UV-Vis, fluorescence and CD spectroscopy (Fig. 3 and 4). By plotting the CD intensity against the temperature, **OPV1** shows a sharp phase transition at 50 °C (Fig. 5) indicating a highly cooperative alteration. The phase transition is fully reversible, however, with a hysteresis of about 10 °C. Fluorescence measurements reveal that the emission of **OPV1** is still quenched²⁴ at a temperature above 50 °C, while the maximum is red shifted compared to that in chloroform. This behaviour indicates that the amphiphiles of

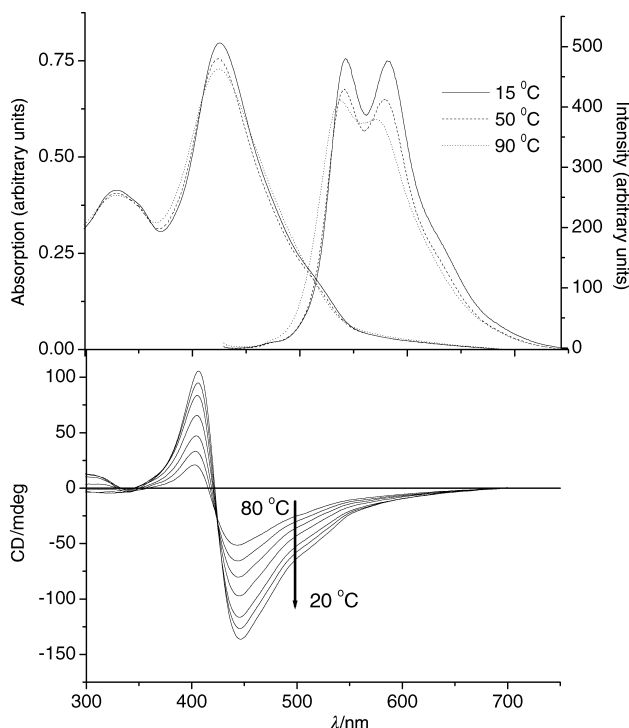


Fig. 4 Temperature dependent a) UV-Vis and fluorescence and b) CD measurements for **OPV2** at $1.6 \times 10^{-5} \text{ mol L}^{-1}$ in water.

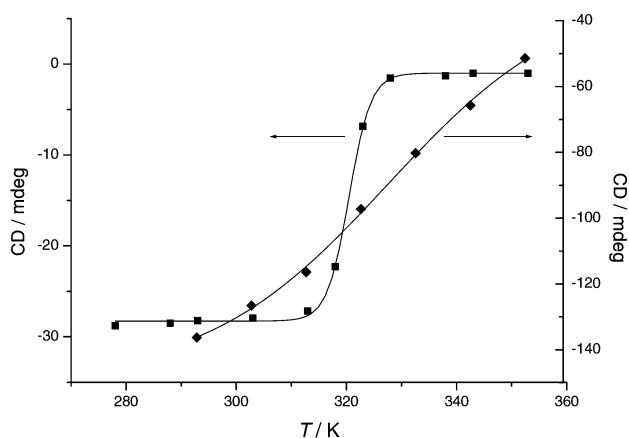


Fig. 5 Change of the Cotton effect of **OPV1** (squares) and **OPV2** (diamonds) in water ($1.6 \times 10^{-5} \text{ mol L}^{-1}$) as a function of temperature and fitted curves.

OPV1 are still aggregated above this transition temperature. The disappearance of the Cotton effect above $50 \text{ }^\circ\text{C}$ shows, however, that the transition is due to the transformation of chiral aggregates into non-chiral, less ordered aggregates. In the UV-Vis spectra, a red shift from $\lambda_{\text{max}} = 400$ to $\lambda_{\text{max}} = 417 \text{ nm}$ is observed upon heating, which could point to conformational changes of the oligomers. Another plausible explanation is that the distance between the oligomers increases in the disordered aggregates resulting in a weaker exciton coupling. Compound **OPV2** displays similar features, but in this case without a sharp phase transition. The Cotton effect, the fluorescence and absorption maxima all show a nearly linear decrease with increasing temperature (Fig. 5). Therefore, we assume that the transition between the well-ordered chiral aggregates and disordered aggregates is a less cooperative process.

The transition of **OPV1** and **OPV2** between the well-ordered chiral aggregates and disordered stacks can be described by the Van't Hoff equation assuming that the number of molecules remains the same in both phases. The equilibrium constants for this transition is given by eqn. (1).

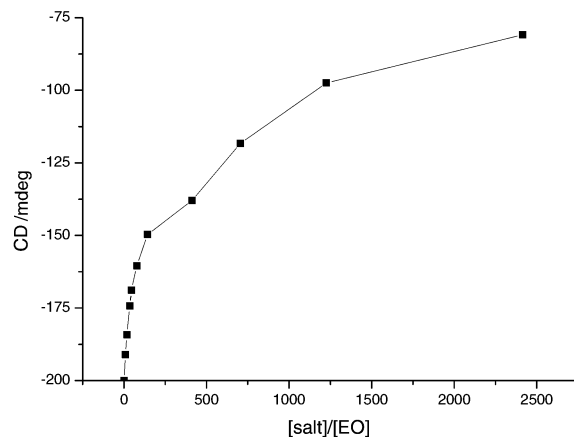


Fig. 6 Change of the Cotton effect of **OPV2** in water ($2.5 \times 10^{-5} \text{ mol L}^{-1}$) as a function of the salt-ethylene oxide (EO) ratio.

$$K_{\text{eq}} = \frac{\text{CD}_{\text{obs}} - \text{CD}_{\text{max}}}{\text{CD}_{\text{min}} - \text{CD}_{\text{obs}}} \quad (1)$$

Evaluation of the temperature dependency of these equilibrium constants yielded the thermodynamic parameters $\Delta H = 165 \text{ kJ mol}^{-1}$ and $\Delta S = 570 \text{ J mol}^{-1} \text{ K}^{-1}$ for **OPV1** and $\Delta H = 35 \text{ kJ mol}^{-1}$ and $\Delta S = 104 \text{ J mol}^{-1} \text{ K}^{-1}$ for **OPV2**. The positive values of ΔS are in agreement with the proposed loss in organisation when going from chiral aggregates to disordered stacks.

The influence of salts on the aggregates formed by our amphiphiles was studied by adding LiClO_4 to a solution of **OPV2** in water. Addition of the salt resulted in a non-linear decrease of the Cotton effect as function of the salt concentration (Fig 6). UV-Vis spectra show a small blue shift (3 nm) upon adding lithium perchlorate. The cations presumably interrupt the packing of the ethylene glycol wedges, hence inducing flexibility between the OPV-oligomers. This interruption results in a decrease of helical order in the supramolecular aggregates.

Based on our optical studies in water, the OPV units are arranged in helical aggregates and shielded from the aqueous solution by the ethylene glycol wedges. In the disordered stacks, the OPV moieties are not helically arranged and, presumably, are free to rotate. The symmetric bolaamphiphile **OPV2** is probably organised in monolayers while **OPV1** is assembled in (interdigitated) bilayers due to its asymmetric nature. **OPV1** behaves as a classical amphiphile in water and shows the typical sharp phase transition found for bilayers. Interestingly, the phase transition temperature of **OPV1** is very close to the melting temperature of this amphiphile in the solid state (*vide infra*). Surprisingly, the properties of **OPV2** are different, a more gradual transition from a chiral aggregate to a disordered stack is observed, which must be due to a modified hydrophilic-hydrophobic balance.

For the preparation of Langmuir monolayers it turned out that the ethylene glycol headgroups are not suitable for obtaining stable layers, presumably due to the introduced intrinsic flexibility by the chosen hydrophilic groups.

Preliminary experiments show that the π -conjugated oligomers can be applied in FET-devices; however, the mobility is low, e.g. at a gate voltage of -100 V an on-current of $0.5 \text{ } \mu\text{A}$ with a mobility of around $10^{-6} \text{ cm}^2 \text{ V}^{-1} \text{ s}^{-1}$ is found. Optimisation of the performance of the devices is underway.

Acknowledgements

J. van Dongen is acknowledged for performing MALDI TOF measurements, K. T. Hoekerd (TNO Institute of Industrial Technology, Materials Technology Division) for assistance with the FET devices and measurements and J. M. Hannink

(University of Nijmegen) for his help with the monolayer experiments. The research of A. P. H. J. Schenning has been made possible by a fellowship of the Royal Netherlands Academy of Arts and Sciences.

References

- 1 W. J. Feast, J. Tsibouklis, K. Pouwer, L. Groenendaal and E. W. Meijer, *Polymer*, 1996, **37**, 5017.
- 2 (a) R. E. Martin and F. Diederich, *Angew. Chem., Int. Ed.*, 1999, **38**, 1350; (b) J. M. Tour, *Chem. Rev.*, 1996, **96**, 537.
- 3 E. Peeters, A. Marcos Ramos, S. C. J. Meskers and R. A. J. Janssen, *J. Chem. Phys.*, 2000, **122**, 9445.
- 4 (a) R. E. Gill, A. Meetsma and G. Hadziioannou, *Adv. Mater.*, 1996, **8**, 212; (b) A. M. van de Craats, J. M. Warman, A. Fechtenkotter, J. D. Brand, M. A. Harbison and K. Müllen, *Adv. Mater.*, 1999, **11**, 1469.
- 5 K. Choudroudis and D. B. Mitzi, *Chem. Mater.*, 1999, **11**, 3028.
- 6 F. S. Schoonbeek, J. H. van Esch, B. Wegewijs, D. B. A. Rep, M. P. de Haas, T. M. Klapwijk, R. M. Kellog and B. L. Feringa, *Angew. Chem., Int. Ed.*, 1999, **38**, 1393.
- 7 (a) A. P. H. J. Schenning, P. Jonkheijm, E. Peeters and E. W. Meijer, *J. Am. Chem. Soc.*, 2001, **123**, 409; (b) A. El-ghayoury, E. Peeters, A. P. H. J. Schenning and E. W. Meijer, *Chem. Commun.*, 2000, 1969.
- 8 (a) G. Widawski, M. Rawiso and B. François, *Nature*, 1994, **369**, 387; (b) M. A. Hempenius, B. M. W. Langeveld-Voss, J. A. E. H. van Haare, R. A. J. Janssen, S. S. Sheiko, J. P. Spatz and M. Möller, *J. Am. Chem. Soc.*, 1998, **120**, 2798.
- 9 (a) F. Hide, M. A. Diaz-García, B. J. Schwartz and A. J. Heeger, *Acc. Chem. Res.*, 1997, **30**, 430; (b) C. J. Drury, C. M. J. Mutsaers, C. M. Hart, M. Matters and D. M. de Leeuw, *Appl. Phys. Lett.*, 1998, **73**, 108.
- 10 (a) F. Vögtle, *Supramolecular Chemistry*, Wiley, New York, 1991, 283; (b) J. H. Fendler, *Membrane Mimetic Chemistry*, Wiley, New York, 1982.
- 11 See for example (a) T. Bjørnholm, D. R. Greve, N. Reitzel, T. Hassnkam, K. Kjaer, P. B. Howes, N. B. Larsen, J. Bogelund, M. Jayaraman, P. C. Ewbank and R. D. McCullough, *J. Am. Chem. Soc.*, 1998, **120**, 7643; (b) L. Belobrzechkaja, G. Bajo, A. Bolognes and M. Catellani, *Synth. Met.*, 1997, **84**, 195; (c) R. D. McCullough and S. P. Williams, *J. Am. Chem. Soc.*, 1993, **115**, 11608; (d) R. D. McCullough and S. P. Williams, *Chem. Mater.*, 1995, **7**, 2001; (e) I. Lévesque and M. Leclerc, *J. Chem. Soc., Chem. Commun.*, 1995, 2293; (f) K. Fäid, M. Fréchette, M. Ranger, L. Mazerolle, I. Lévesque, M. Leclerc, T.-A. Chen and R. D. Rieke, *Chem. Mater.*, 1995, **8**, 2843.
- 12 A. F. M. Kilbinger, A. P. H. J. Schenning, F. Goldoni, W. J. Feast and E. W. Meijer, *J. Am. Chem. Soc.*, 2000, **122**, 1820.
- 13 A. F. M. Kilbinger and W. J. Feast, *J. Mater. Chem.*, 2000, **10**, 1777.
- 14 (a) V. Urban, H. H. Wang, P. Thiyagarajan, K. C. Littrell, H. B. Wang and L. Yu, *J. Appl. Crystallogr.*, 2000, **33**, 645; (b) H. Xiong, L. Qin, J. Sun, X. Zhang and J. Shen, *Chem. Lett.*, 2000, **35**, 586.
- 15 Z. Bo, C. Zhang, N. Severin, J. Rabe and A. D. Schlüter, *Macromolecules*, 2000, **33**, 2688.
- 16 (a) A. P. H. J. Schenning, E. Peeters and E. W. Meijer, *J. Am. Chem. Soc.*, 2000, **122**, 4489; (b) D. T. Balogh, A. Dhanabalan, P. Dynarowicz-Latka, A. P. H. J. Schenning, O. N. Oliveira, Jr., E. W. Meijer and R. A. J. Janssen, *Langmuir*, 2001, **17**, 3281.
- 17 V. Cimrová, M. Remmers, D. Neher and G. Wegner, *Adv. Mater.*, 1996, **8**, 146.
- 18 A. P. H. J. Schenning, A. El-ghayoury, E. Peeters and E. W. Meijer, *Synth. Met.*, 2001, **121**, 1253.
- 19 (a) A. R. A. Palmans, J. A. J. M. Vekemans, E. E. Havinga and E. W. Meijer, *Angew. Chem., Int. Ed. Engl.*, 1997, **36**, 2648; (b) J. Sandström, *Circular Dichroism: principles and applications*, Eds. K. Nakanishi, N. Berova, and R. Woodey, VCH, Weinheim, 1994.
- 20 S. C. J. Meskers, E. Peeters, B. M. W. Langeveld-Voss and R. A. J. Janssen, *Adv. Mater.*, 2000, **12**, 589.
- 21 E. Peeters, P. A. van Hal, J. Knol, C. J. Brabec, N. S. Sariciftci, J. C. Hummelen and R. A. J. Janssen, *J. Phys. Chem. B*, 2000, **104**, 10174.
- 22 R. Fiesel and U. Scherf, *Acta Polym.*, 1998, **49**, 445.
- 23 B. M. W. Langeveld-Voss, D. Beljonne, Z. Shuai, R. A. J. Janssen, S. C. J. Meskers, E. W. Meijer and J. L. Brédas, *Adv. Mater.*, 1998, **10**, 1343.
- 24 The critical aggregation concentration (c.a.c.) could not be determined since the optical techniques were not sensitive enough to measure more diluted concentrations than 10^{-7} mol L⁻¹.